Wind Field Disturbance Analysis and Flight Control System Design for a Novel Tilt-Rotor UAV

QIAN ZHANG[1], JINGJUAN ZHANG[2], XUEYUN WANG[2], YIFAN XU[2], AND ZELONG YU[2]
[1]School of Aeronautic Science and Engineering, Beihang University, Beijing 100191, China
[2]School of Instrumentation Science and Optoelectronics Engineering, Beihang University, Beijing 100191, China

Corresponding author: Jingjuan Zhang (zhangjingjuan@buaa.edu.cn)

ABSTRACT The wind field has a great influence on the control stability of Tilt-rotor unmanned aerial vehicle (UAV), especially during the take-off and landing phase. The airspeed of UAV is so small during these phases that it cannot generate stable aerodynamic forces, which will significantly reduce the wind robustness of Tilt-rotor UAV. In this article, the disturbance of wind field is analyzed from two perspectives: the wind field acting on the UAV fuselage, which is regarded as external interference, and the wind acting on the propeller, which is considered as modeling error. After analyzing the interference mechanism of wind field, a generalized extended state observer (GESO) and a $H\infty$ robust control method with mixed sensitivity are proposed, which could empower the Tilt-rotor UAV with good interference suppression ability as well as better performance tracking ability. Finally, the laboratory simulation and flight experiment are studied. The results validate the theory and prove that the proposed method could resist the interference of wind field and shows excellent control effect.

INDEX TERMS Tilt-rotor, unmanned aerial vehicle, wind field disturbance, generalized extended state observer, robust control.

I. INTRODUCTION

Integrating the advantages of fixed-wing aircraft and helicopter, the Tilt-rotor unmanned aerial vehicle (UAV) has received wide attention with the development of aviation industry [1]–[4]. With the tiltable rotor nacelle system, the Tilt-rotor UAV could provide the power of variable vector for hover and level flight, which allows the Tilt-rotor UAV to have greater load capacity, longer cruising time and better adaptability to take-off and landing sites [5]–[7]. However, with unique structural characteristics, the Tilt-rotor UAV has more complex features than traditional aircraft. For example, the interaction between rotor and wing makes Tilt-rotor UAV a strong nonlinear and coupling system [8]–[10], besides this, the multiple actuators make the control strategy even more complex, and so on [11], [12].

Taking these challenges into consideration, many scholars have conducted numerous related studies in the simulation environment [9], [11], [13]–[19]. Regarding the nonlinear control problem of Tilt-rotor electrical vertical take-off and landing, [13] discussed a hovering state

The associate editor coordinating the review of this manuscript and approving it for publication was Dipankar Deb.

attitude control law based on nonlinear dynamic inversion, and successfully implemented and evaluated the proposed method in a proof of concept simulation. To deal with the actuator saturation and uncertain disturbance problems of a novel Tilt-rotor UAV, [14] proposed an improved control method based on the combination of the robust servo linear quadratic regulator optimal control and the extended state observer. Flight simulations were carried out to verify the effectiveness of the designed flight control law. In order to solve the problem of manipulation redundancy in conversion mode, [15] proposed a novel tilting strategy based on Ant Colony Optimization (ACO), and found the optimal tilting path in the conversion corridor. The test results showed that the proposed method could effectively solve the manipulation redundancy in the conversion mode. In [16], the modeling and control technology of Bell-XV15 were studied. A nonlinear hierarchical control strategy was adopted to provide automatic hover control of the tiltrotor aircraft. In [17], a nonlinear dynamic model had been developed based on a component buildup methodology and the lifting-line theory for a novel Tilt-rotor UAV, and the results obtained through simulations were satisfactory. A quadratic-programming-based optimal control method was developed based on a Tilt-rotor

time-varying linear model in [18], then, three typical tilting transition missions were simulated using the nonlinear model of XV-15 Tilt-rotor aircraft.

These researches have improved the flight performance of the Tilt-rotor UAV, however, most of the related studies focus on the simulation phase, while the mechanism of wind field interference at low airspeed is rarely studied. During the vertical take-off and landing phase, the rotor nacelle system tilts to vertical position and works like a helicopter, the attitude and position of Tilt-rotor are controlled by direct force of rotor system. During these phases, the airspeed is so small that it cannot generate stable aerodynamic forces, and the aerodynamic interference which caused by wind field will reduce the stability of the aircraft [9], [20]–[22]. In [9], the rotor-wing aerodynamic interaction of a scaled V-22 Osprey Tilt-rotor in the helicopter mode was studied by computational fluid dynamics (CFD) numerical simulation. However, the wind field was assumed to be zero and was not considered in the modeling in this article. In [20], the wind-gusts were introduced into the modeling as external disturbances, then, a model predictive controller (MPC) for attitude maneuvers of Tilt-rotor was proposed. Due to the simple structure of tilt rotor in this article, the influence of wind field was relatively small and the simulation results had high accuracy. In addition to the influence of the wind field on the stability of the fuselage, the wind field could change the direction of incoming flow of propeller, which will interfere with the pull output of rotor propeller. A relative wind model was added to the aerodynamic modeling of propeller in [22], however, the researchers did not further study the effect of wind on Tilt-rotor control.

In this article, the research focuses on the wind disturbance and control system design of Tilt-rotor UAV during the vertical take-off and landing phase. A number of control strategies have been proposed to deal with the problems of external disturbances and parametric uncertainties, such as sliding model control [23]–[25], model predictive control [26], [27], neural network control [28]–[31], and so on. Sliding mode control (SMC) strategy has been widely used because of its characteristic of insensitivity to disturbance, however, the sign function of SMC is easy to cause inevitable oscillations in the system. For example, in [25], a robust nonlinear controller which combines the sliding mode control technique and the back-stepping control technique was proposed to deal with model uncertainty and external disturbances. However, the sliding mode control did lead to inevitable oscillations. A predictor-based model predictive control method is applied for the roll and yaw control of a rudderless quad-tiltrotor UAV [27], the simulation results and final flight tests confirmed that the predictor-based adaptive controller could effectively improve the roll and yaw control quality of the tested quad-tiltrotor model. However, the external disturbances were not considered in the design of the control methods. In [31], the neural network theory was combined with sliding mode control, which could enhance the adaptive capability of the dynamic system. The results

did show remarkable stability and dynamic performance, however, the introduction of neural network increased the computational complexity and burden of the controller. During the vertical take-off and landing phase of Tilt-rotor UAV, the disturbance of wind field is considered from external compound disturbance and parametric uncertainties simultaneously, which makes the situation more challenging. The characteristics of high computational complexity and slow convergence of these control methods may result in the decline of the dynamic performance of the controlled object in practical applications. Therefore, it is still a challenging and meaningful task to construct an effective control algorithm in practical application of Tilt-rotor UAV.

$H\infty$ robust control method could empower the controller with robust performance by optimizing the infinite norm of some performance indexes in $H\infty$ space (Hardy space), which allows the system to have good interference suppression and better tracking performance, and it has been widely applied in UAV control [32]–[34]. In [32], an attitude controller for a Tilt-wing UAV was designed, which used the $H\infty$ synthesis to minimize $H\infty$ norm from the disturbance and noise to the estimation error. Then, a simulation containing certain disturbances and noises was conducted to verify the performance and robustness of the controller, which met the requirements. In [33], in order to ensure the stability of the morphing UAV during the wings change, $H\infty$ robust control method was designed and the simulation and semi-physical results showed that it could suppress external interference caused by changes of structure. What's more, for the uncertainty of external disturbance, the extended state observer (ESO) can not only recover the system state but also estimate all the disturbances in real time [35]–[38]. In order to estimate the disturbances and uncertainties that affect the system, an ESO was proposed in [35], and then the estimated results were used for feedback linearization and embedded model control system, and good control accuracy was obtained. In [38], an improved ESO based on sigmoid function was proposed to estimate the model uncertainties and external disturbance caused by the large attitude maneuver and complicated external environment during the re-entry phase of the reusable launch vehicle (RLV). The simulation results showed that the ESO could accurately and quickly estimate the interference of the nonlinear RLV system.

Therefore, in this article, after analyzing the interference mechanism of wind field, a generalized extended state observer (GESO) and control method based on $H\infty$ robust control with mixed sensitivity are proposed. The algorithm is implemented and evaluated with simulation experiment and actual flight verification. The main contributions of this work can be summarized as following:

(1) Two aspects of the wind field disturbance are analyzed: the wind field acting on the UAV fuselage, which is regarded as external interference, and the wind acting on the propeller, which is considered as a modeling error.
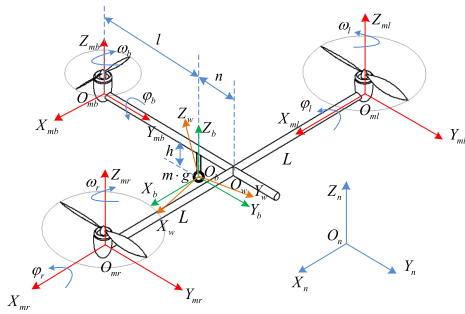
FIGURE 1. The coordinate systems of Tilt-rotor UAV.

(2) A generalized extended state observer is designed to estimate the interference force and torque, and the stability of GESO is analyzed.

(3) To deal with the external disturbance and internal modeling error caused by wind field, a $H\infty$ robust control with mixed sensitivity is proposed, which could bring better interference suppression ability and performance tracking ability to the system.

The article is organized as follows: Section II presents the complete model of the Tilt-rotor UAV, including the rotor propeller and interference mechanism of wind field. Section III introduces the GESO and its stability is proved by the Lyapunov theory. Then, the method of mixed sensitivity $H\infty$ robust control is proposed for wind resistance control. Comparative simulation and experiment results are provided and discussed in Section IV. Followed by conclusion in Section V.

II. MODEL FOR NOVEL TILT_ROTOR UAV

A. DEFINITION OF COORDINATE SYSTEMS

The novel Tilt-rotor UAV studied in this article is mainly powered by two tiltable rotors at both ends of the wings. A ducted fan is equipped at the end of UAV to maintain the stability of pitch attitude during take-off and landing. As shown in Figure 1, the coordinate systems are defined as follows: $O_b - X_bY_bZ_b$ is the body frame. Where O_b is at the center of gravity and it is the original point of Tilt-rotor UAV, X_b pointing to the right of the UAV, Y_b pointing front and Z_b pointing up. $O_n - X_nY_nZ_n$ is the navigation frame which coincides with the geographic frame (east, north, upwards). $O_{mr} - X_{mr}Y_{mr}Z_{mr}$, $O_{ml} - X_{ml}Y_{ml}Z_{ml}$, $O_{mb} - X_{mb}Y_{mb}Z_{mb}$ are the motor frames which are fixed with three motors, respectively. Referring to the center of gravity, the coordinate of right motor is $[L, n, h]^T$, the left one's is $[-L, n, h]^T$ and the rear one's is $[0, -l, h]^T$.

The relationship between body frame and navigation frame can be described by attitude rotation matrix:

$$C_n^b = R_y(\phi)R_x(\theta)R_z(\psi)$$
$$= \begin{bmatrix} \cos\phi & 0 & -\sin\phi \\ 0 & 1 & 0 \\ \sin\phi & 0 & \cos\phi \end{bmatrix} \begin{bmatrix} 1 & 0 & 0 \\ 0 & \cos\theta & \sin\theta \\ 0 & -\sin\theta & \cos\theta \end{bmatrix}$$

$$\times \begin{bmatrix} \cos\psi & \sin\psi & 0 \\ -\sin\psi & \cos\psi & 0 \\ 0 & 0 & 1 \end{bmatrix} \quad (1)$$

where ϕ, θ, ψ represent the roll, pitch and yaw angle, respectively.

As there is only one degree of freedom for each motor, the relationship between motor frame and body frame can be established by the tilt angle. For three motors, the tilt angles of vertical state are 90°. From the rear view, it is 0° when the tail motor tilts left to horizontal. From the right view, it is 0° when the right and left motors tilt front to horizontal. Then, take the right motor as an example:

$$C_{mr}^b = R_x(90° - \varphi_r) = \begin{bmatrix} 1 & 0 & 0 \\ 0 & \sin\varphi_r & \cos\varphi_r \\ 0 & -\cos\varphi_r & \sin\varphi_r \end{bmatrix} \quad (2)$$

B. DYNAMIC MODEL

Dynamic equation of rigid body motion can be established according to Newton's law of motion and the Euler equation.

The Newton equation with respect to the navigation coordinate frame can be written as:

$$m\ddot{X} = F^n \quad (3)$$

where $X = [x, y, z]^T$ is the navigation position vector, $m \in R$ is the mass of Tilt-rotor UAV, F^n is the external force in navigation frame.

The thrust of each motor can be defined as $T_r^{mr} = [0, 0, T_r]^T$, $T_l^{ml} = [0, 0, T_l]^T$, $T_b^{mb} = [0, 0, T_b]^T$ in motor frame, respectively. Translate the thrusts vector into body frame

$$\begin{cases} T_r^b = C_{mr}^b T_r^{mr} \\ T_l^b = C_{ml}^b T_l^{ml} \\ T_b^b = C_{mb}^b T_b^{mb} \end{cases} \quad (4)$$

The gravity can be defined as $G^n = [0, 0, -mg]^T$, in addition to the interference caused by the external environment, the resultant force in navigation frame can be described as

$$F^n = C_b^n(T_r^b + T_l^b + T_b^b + F_d^b) + G^n \quad (5)$$

where F_d^b is the disturbance caused by external environment, and C_b^n is transpose matrix of C_n^b. Thus, the full expression of translational dynamic equations is defined as (6), as shown at the bottom of the next page.

The Euler equation with respect to the body coordinate frame can be written as

$$I\dot{\omega} + \omega \times I\omega = M^b \quad (7)$$

where $I \in \mathbb{R}^{3\times3}$ is an inertia matrix and ω is the body angular velocity vector.

For UAVs, generally, cross products of inertia can be ignored, and the Eq. (7) can be redefined as

$$\begin{cases} M_x^b = I_{xx}\dot{\omega}_x^b - (I_{yy} - I_{zz})\omega_y^b\omega_z^b \\ M_y^b = I_{yy}\dot{\omega}_y^b - (I_{zz} - I_{xx})\omega_z^b\omega_x^b \\ M_z^b = I_{zz}\dot{\omega}_z^b - (I_{xx} - I_{yy})\omega_x^b\omega_y^b \end{cases} \quad (8)$$

where M_x^b, M_y^b and M_z^b are the components of vector M^b.

As mentioned above, the coordinates of three motors are $d_r = [L, n, h]^T$, $d_l = [-L, n, h]^T$ and $d_b = [0, -l, h]^T$. So the torques which are derived based on the thrusts of three motors can be defined as (9), as shown at the bottom of the next page.

The relationship between angular velocity vector and Euler angles can be described as

$$
\begin{bmatrix} \dot{\phi} \\ \dot{\theta} \\ \dot{\psi} \end{bmatrix} = \begin{bmatrix} \sin\phi\tan\theta & 1 & -\cos\phi\tan\theta \\ \cos\phi & 0 & \sin\phi \\ -\sin\phi/\cos\theta & 0 & \cos\phi/\cos\theta \end{bmatrix} \begin{bmatrix} \omega_x^b \\ \omega_y^b \\ \omega_z^b \end{bmatrix}
$$

$$(10)$$

Then the dynamic model of Tilt-rotor UAV in take-off and landing phase can be summarized as follows (11), as shown at the bottom of the page 6

C. MECHANISM OF WIND DISTURBANCE

The interference of wind field is mainly reflected on two aspects. On one side, the wind field produces aerodynamic resistance, causing interference force and torque on the fuselage of UAV. On the other hand, the incoming flow of propeller is influenced by wind field and it has an effect on motor thrust.

1) THE INFLUENCE OF WIND FIELD ON THE FUSELAGE

In the take-off, landing or hovering state, the interference force and torque generated by the wind field can be analyzed from the perspective of atmospheric resistance. The atmospheric resistance can be described as

$$
F_w^b = \mathrm{sgn}\left(V_w^b\right) \cdot \frac{1}{2} c\rho S \left(V_w^b\right)^2 \tag{12}
$$

where $c = \begin{bmatrix} c_x & 0 & 0 \\ 0 & c_y & 0 \\ 0 & 0 & c_z \end{bmatrix}$ is the coefficient matrix atmospheric

resistance, $S = \begin{bmatrix} S_x & 0 & 0 \\ 0 & S_y & 0 \\ 0 & 0 & S_z \end{bmatrix}$ is the matrix of windward area,

$\mathrm{sgn}\left(V_w^b\right) = \begin{bmatrix} \mathrm{sgn}\left(V_{wx}^b\right) \\ \mathrm{sgn}\left(V_{wy}^b\right) \\ \mathrm{sgn}\left(V_{wz}^b\right) \end{bmatrix}$ represents the direction of wind

speed.

The atmospheric resistance is acting on the UAV's geometric center, it will produce interference torque relative to the center of gravity

$$
M_w^b = F_w^b \times R \tag{13}
$$

where R is the vector between centroid and center of gravity.

2) THE INFLUENCE OF WIND FIELD ON THE PROPELLER

In order to simplify the structure, the Tilt-rotor UAV researched in this article uses the fixed pitch propeller. As shown in Figure 2, the influence of the wind field on the propeller is mainly reflected in the change of the angle of attack.

In Figure 2, V_I is the incoming flow speed, $U_a = \sqrt{(\omega r_p)^2 + V_I^2}$ is the flow velocity relative to the propeller, $\phi_p = \tan^{-1}(\frac{V_I}{\omega r_p})$ is the flow angle, β_p is the propeller blade angle, $\alpha_p = \beta_p - \tan^{-1}(\frac{V_I}{\omega r_p})$ is the attack angle of propeller. Generally, there is no aerodynamic force in the hub, which accounts for about 20% of the total propeller diameter. Therefore, the leaf element at $0.4r$ is selected as the research object, and $r_p = 0.4r$.

According to the blade element theory, the profile of the propeller can be taken as a small wing, the lift and drag can be described as

$$
dL = \frac{1}{2}\rho U_a^2 \alpha_p L_p ds \tag{14}
$$

$$
dD = \frac{1}{2}\rho U_a^2 \alpha_p D_p ds \tag{15}
$$

where L_p and D_p are pull and drag coefficient, ρ is the air density, ds is a small blade area. Then, the forward pull and rotation resistance in motor frame are

$$
dT_z = dL\cos\phi_p - dD\sin\phi_p \tag{16}
$$

$$
dT_y = dL\sin\phi_p + dD\cos\phi_p \tag{17}
$$

Combining with the expression of each variable, the pull of this small blade can be rewrite as

$$
dT_z = \frac{1}{2}\rho L_p ds\sqrt{(\omega r_p)^2 + V_I^2}\,\omega r_p \alpha_p
$$
$$
- \frac{1}{2}\rho D_p ds\sqrt{(\omega r_p)^2 + V_I^2}\,V_I \alpha_p \tag{18}
$$

The size of the propeller used on this Tilt-rotor UAV is 910×303mm, the propeller blade angle at this leaf element

$$
\begin{cases}
\ddot{x} = \frac{1}{m}\begin{pmatrix} \left(-T_b\cos\varphi_b + F_{dx}^b\right)\cdot(\cos\phi\cos\psi - \sin\phi\sin\theta\sin\psi) - (T_r\cos\varphi_r + T_l\cos\varphi_l + F_{dy}^b)\cdot(\cos\theta\sin\psi) \\ + (T_r\sin\varphi_r + T_l\sin\varphi_l + T_b\sin\varphi_b + F_{dz}^b)\cdot(\sin\phi\cos\psi + \cos\phi\sin\theta\sin\psi) \end{pmatrix} \\
\ddot{y} = \frac{1}{m}\begin{pmatrix} \left(-T_b\cos\varphi_b + F_{dx}^b\right)\cdot(\cos\phi\sin\psi + \sin\phi\sin\theta\cos\psi) + (T_r\cos\varphi_r + T_l\cos\varphi_l + F_{dy}^b)\cdot(\cos\theta\cos\psi) \\ + (T_r\sin\varphi_r + T_l\sin\varphi_l + T_b\sin\varphi_b + F_{dz}^b)\cdot(\sin\phi\sin\psi - \cos\phi\sin\theta\cos\psi) \end{pmatrix} \\
\ddot{z} = \frac{1}{m}\begin{pmatrix} \left(-T_b\cos\varphi_b + F_{dx}^b\right)\cdot(-\sin\phi\cos\theta) + (T_r\cos\varphi_r + T_l\cos\varphi_l + F_{dy}^b)\cdot(\sin\theta) \\ + (T_r\sin\varphi_r + T_l\sin\varphi_l + T_b\sin\varphi_b + F_{dz}^b)\cdot(\cos\phi\cos\theta) - mg \end{pmatrix}
\end{cases} \tag{6}
$$

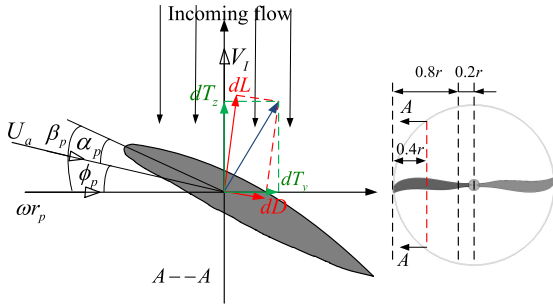**FIGURE 2.** The profile of propeller.

can be calculated as $\beta_p = \tan^{-1}\frac{303}{2\pi \times 910/2 \times 0.6} \approx 0.177rad$. As the blade angle of attack need to be positive, then

$$\tan^{-1}(\frac{V_I}{\omega r_p}) < 0.177rad \Rightarrow \frac{V_I}{\omega r_p} < 0.177 \qquad (19)$$

Define $\delta_L = \frac{1}{2}\rho L_p ds$ and $\delta_D = \frac{1}{2}\rho D_p ds$, the pull of this small blade can be simplified as

$$dT_z = \delta_L(\omega r_p)^2 \beta_p - \delta_L \omega r_p V_I - \delta_D \omega r_p V_I \beta_p + \delta_D V_I^2 \qquad (20)$$

As shown in Eq. (20), the thrust of propeller will be affected by quadratic speed of the wind field, thus the influence of this part of the wind field should be built into the dynamic model.

III. DESIGN OF WIND RESISTANT CONTROLLER
As in the take-off and landing phase, the horizontal attitudes are controlled in a very small range and the tilt angles of right and left motors are kept in the vertical state. To provide the yaw moment, the rear motor has to keep a small tilt angle. Therefore, considering the Eq. (10) $\sim$ Eq. (13) and Eq. (20), the control model of take-off and landing phase can be simplified as

$$\begin{cases} \dot{x} = Ax + Bu + B_d d \\ y = Cx \end{cases} \qquad (21)$$

where $x = \begin{bmatrix} h & \theta & \phi & \psi & V_z & \omega_x & \omega_y & \omega_z \end{bmatrix}^T$, $u = \begin{bmatrix} T_r & T_l & T_b & \varphi_b \end{bmatrix}^T$, $y = \begin{bmatrix} h & \theta & \phi & \psi \end{bmatrix}^T$, $d = \begin{bmatrix} F_{dz}^b & M_{dx}^b & M_{dy}^b & M_{dz}^b \end{bmatrix}^T$. $A = \begin{bmatrix} O_{4\times4} & I_4 \\ O_{4\times4} & O_{4\times4} \end{bmatrix}$, $B = \begin{bmatrix} O_{4\times4} \\ 1/m & 1/m & 1/m & 0 \\ n/I_{xx} & n/I_{xx} & -l/I_{xx} & 0 \\ -L/I_{yy} & L/I_{yy} & 0 & 0 \\ 0 & 0 & -\varphi_b l/I_{zz} & -T_b l/I_{zz} \end{bmatrix}$,

$$C = \begin{bmatrix} I_4 \\ O_{4\times4} \end{bmatrix}, B_d = \begin{bmatrix} O_{4\times4} \\ 1/m & 0 & 0 & 0 \\ 0 & 1/I_{xx} & 0 & 0 \\ 0 & 0 & 1/I_{yy} & 0 \\ 0 & 0 & 0 & 1/I_{zz} \end{bmatrix}. O_{4\times4}$$

denotes zero matrices with dimension of 4×4 and I_4 denotes fourth-order identity matrix.

In this part, a $H\infty$ robust control method with GESO is proposed, and the configuration of control method is shown in Figure 3.

A. DESIGN OF GENERALIZED EXTENDED STATE OBSERVER AND STABILITY ANALYSIS
The attitude feedback information of the controller is calculated by micro electro mechanical system (MEMS) and GPS. However, the angular velocity information obtained from MEMS contains large noise, which will affect the performance of the controller. What's more, the interference mechanism of wind field has been researched before, but the actual wind field is difficult to measure and model in real-time. State observer is an effective way to solve this problem. In general, the GESO is used to estimate system states and total disturbances with less dependence on model information [39], [40]. In this section, a GESO is designed to estimate the states and the disturbances that are difficult to measure, then, the stability of GESO is proved by the Lyapunov theory.

Define the extended state $\bar{x} = \begin{bmatrix} x & d \end{bmatrix}^T$, the GESO can be designed as

$$\begin{cases} \dot{\hat{\bar{x}}} = \bar{A}\hat{\bar{x}} + \bar{B}u + L\left(y - \hat{y}\right) \\ \hat{y} = \bar{C}\hat{\bar{x}} \end{cases} \qquad (22)$$

where $\bar{A} = \begin{bmatrix} A & B_d \\ O_{4\times8} & O_{4\times4} \end{bmatrix}$, $\bar{B} = \begin{bmatrix} B \\ O_{4\times4} \end{bmatrix}$, $\bar{C} = \begin{bmatrix} C & O_{4\times4} \end{bmatrix}$. $\hat{\bar{x}} = \begin{bmatrix} \hat{x} & \hat{d} \end{bmatrix}^T$ is the estimate value of extended state and $L \in \mathbb{R}^{12\times4}$ is the observe gain matrices that need to be designed.

Then, define the estimation error as $e = \bar{x} - \hat{\bar{x}}$, and the dynamic equation of e can be expressed as

$$\dot{e} = \left(\bar{A} - L\bar{C}\right)e + Eh \qquad (23)$$

where $h = \dot{d}$ is the derivative of external interference, E is the coefficient matrix.

It is clear that if the gain coefficient L could make $\left(\bar{A} - L\bar{C}\right)$ is a Hurwitz matrix, the estimation error will be bounded under the condition that h is bounded. In order to prove the stability of the state observer, the Lyapunov

$$M_m^b = d_r \times T_r^b + d_l \times T_l^b + d_b \times T_b^b + M_d^b$$
$$= \begin{bmatrix} T_r \sin\varphi_r n - T_r \cos\varphi_r h + T_l \sin\varphi_l n - T_l \cos\varphi_l h - T_b \sin\varphi_b l + M_{dx}^b \\ -T_r \sin\varphi_r L + T_l \sin\varphi_l L - T_b \cos\varphi_b h + M_{dy}^b \\ T_r \cos\varphi_r L - T_l \cos\varphi_l L - T_b \cos\varphi_b l + M_{dz}^b \end{bmatrix} \qquad (9)$$
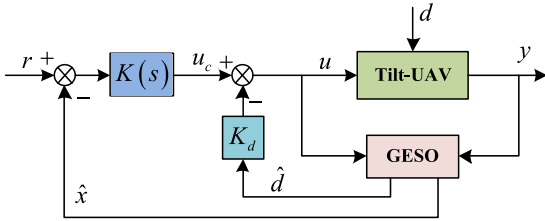
FIGURE 3. The structure of control system based on GESO.

FIGURE 4. System architecture of pitch angle control channel.

function is defined as

$$V = e^T Pe \qquad (24)$$

The time derivative of Lyapunov function is

$$\dot{V} = e^T \left(\left(\bar{A} - L\bar{C} \right)^T P + P \left(\bar{A} - L\bar{C} \right) \right) e + h^T E^T Pe + e^T PEh \qquad (25)$$

As the $\left(\bar{A} - L\bar{C} \right)$ is a Hurwitz matrix, there exists a positive definite symmetric matrix P satisfying

$$\left(\bar{A} - L\bar{C} \right)^T P + P \left(\bar{A} - L\bar{C} \right) = -C_V I_{12} \quad (C_V > 0) \qquad (26)$$

Therefore, the Eq. (25) can be rewritten as

$$\begin{aligned}
\dot{V} &= -e^T \left(C_V I_{12} \right) e + h^T E^T Pe + e^T PEh \\
&\leq -C_V \|e\| \cdot \|e\| + \|Eh\| \cdot \|P\| \cdot \|e\| + \|e\| \cdot \|P\| \cdot \|Eh\| \\
&= -\|e\| \cdot \left(C_V \|e\| - 2 \|Eh\| \cdot \|P\| \right) \\
&\leq -\|e\| \cdot \left(C_V \|e\| - 2\lambda \cdot \gamma \right) \qquad (27)
\end{aligned}$$

where γ is the 2-norm of P, and $\|Eh\| \leq \lambda$. It can be seen that $\dot{V} < 0$, if $\|e\| > \frac{2\lambda \cdot \gamma}{C_V}$, which implies that $\|e\|$ decreases for any e.

IV. $H\infty$ ROBUST CONTROL

The Tilt-rotor UAV works in multi-state and there is mutual interference between the rotors and the wings, therefore, the uncertainty error of modeling results in great difference between the reference model and the actual control system. In addition, the atmospheric disturbance model is based on
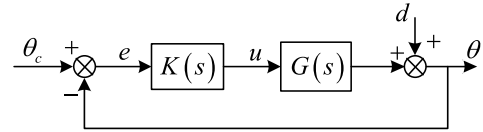
statistical theory, which has large model errors. Therefore, there are problems of system model uncertainty and environmental interference to be considered in the control system of Tilt-rotor UAV. In this article, a control method based on $H\infty$ robust control with mixed sensitivity is proposed, which could bring better interference suppression ability and performance tracking ability to the system [41]–[43].

Take the pitch angle control channel as an example, as shown in Figure 4, θ_c is the reference input, u is the control input, e is the tracking error, $K(s)$ is the controller and d is the external interference.

The transfer functions for θ_c to e, u, θ can be described as

$$S(s) = \frac{e(s)}{\theta_c(s)} = (I + L(s))^{-1} \qquad (28)$$

$$R(s) = \frac{u(s)}{\theta_c(s)} = K(s)(I + L(s))^{-1} \qquad (29)$$

$$T(s) = \frac{y(s)}{\theta_c(s)} = L(s)(I + L(s))^{-1} = I - S(s) \qquad (30)$$

where $L(s) = G(s)K(s)$ is the open loop transfer function of the pitch angle control channel. $S(s)$ is called the sensitivity function and its singular value determines the anti-interference ability of the control system, $T(s)$ is called the complementary sensitivity function and its singular value determines the tracking ability of the control system. In order for the system to have good interference suppression ability and performance tracking ability, the singular values of $S(s)$ and $T(s)$ need to be minimum. However, $S(s) + T(s) = I$ and it is clear that they cannot be minimum at the same time. Therefore, the weighting functions of $W_S(s)$ and $W_T(s)$ are

$$\begin{cases}
\ddot{x} = \frac{1}{m} \begin{pmatrix} \left(-T_b \cos \varphi_b + F_{dx}^b \right) \cdot \left(\cos \phi \cos \psi - \sin \phi \sin \theta \sin \psi \right) - \left(T_r \cos \varphi_r + T_l \cos \varphi_l + F_{dy}^b \right) \cdot \left(\cos \theta \sin \psi \right) \\ + \left(T_r \sin \varphi_r + T_l \sin \varphi_l + T_b \sin \varphi_b + F_{dz}^b \right) \cdot \left(\sin \phi \cos \psi + \cos \phi \sin \theta \sin \psi \right) \end{pmatrix} \\
\ddot{y} = \frac{1}{m} \begin{pmatrix} \left(-T_b \cos \varphi_b + F_{dx}^b \right) \cdot \left(\cos \phi \sin \psi + \sin \phi \sin \theta \cos \psi \right) + \left(T_r \cos \varphi_r + T_l \cos \varphi_l + F_{dy}^b \right) \cdot \left(\cos \theta \cos \psi \right) \\ + \left(T_r \sin \varphi_r + T_l \sin \varphi_l + T_b \sin \varphi_b + F_{dz}^b \right) \cdot \left(\sin \phi \sin \psi - \cos \phi \sin \theta \cos \psi \right) \end{pmatrix} \\
\ddot{z} = \frac{1}{m} \begin{pmatrix} \left(-T_b \cos \varphi_b + F_{dx}^b \right) \cdot \left(-\sin \phi \cos \theta \right) + \left(T_r \cos \varphi_r + T_l \cos \varphi_l + F_{dy}^b \right) \cdot \left(\sin \theta \right) \\ + \left(T_r \sin \varphi_r + T_l \sin \varphi_l + T_b \sin \varphi_b + F_{dz}^b \right) \cdot \left(\cos \phi \cos \theta \right) - mg \end{pmatrix} \\
\dot{\omega}_x^b = \frac{1}{I_{xx}} \left(T_r \sin \varphi_r n - T_r \cos \varphi_r h + T_l \sin \varphi_l n - T_l \cos \varphi_l h - T_b \sin \varphi_b l + M_{dx}^b + (I_{yy} - I_{zz}) \omega_y^b \omega_z^b \right) \\
\dot{\omega}_y^b = \frac{1}{I_{yy}} \left(-T_r \sin \varphi_r L + T_l \sin \varphi_l L - T_b \cos \varphi_b h + M_{dy}^b + (I_{zz} - I_{xx}) \omega_z^b \omega_x^b \right) \\
\dot{\omega}_z^b = \frac{1}{I_{zz}} \left(T_r \cos \varphi_r L - T_l \cos \varphi_l L - T_b \cos \varphi_b l + M_{dz}^b + (I_{xx} - I_{yy}) \omega_x^b \omega_y^b \right)
\end{cases} \qquad (11)$$

Description	Parameter	Value (unite)
Mass	m	$67kg$
Pitch inertia	I_{xx}	$14.49kg \cdot m^2$
Roll inertia	I_{yy}	$42.02kg \cdot m^2$
Yaw inertia	I_{zz}	$54.76kg \cdot m^2$
Right motor coordinates	d_r	$\begin{bmatrix} 1.75 & 0.05 & 0.03 \end{bmatrix}^T m$
Left motor coordinates	d_l	$\begin{bmatrix} -1.75 & 0.05 & 0.03 \end{bmatrix}^T m$
Back motor coordinates	d_b	$\begin{bmatrix} 0 & -0.852 & 0.03 \end{bmatrix}^T m$

defined and a performance index function is proposed as

$$\sup \left(\|W_s (j\omega) S (j\omega)\|^2 + \|W_T (j\omega) T (j\omega)\|^2 \right) < \gamma^2 \quad (31)$$

where γ is a small positive value, $W_S (s)$ and $W_T (s)$ have large values in different frequency bands. In this way, the singular values of $S (s)$ and $T (s)$ can obtain the minimum values in the corresponding frequency band, which gives the $H\infty$ robust control both good interference suppression ability and better performance tracking ability.

V. SIMULATIONS AND EXPERIMENTS

A. SIMULATION RESULTS

The simulation test is performed before the actual flight verification. The Tilt-UAV parameters are shown in table 1.

In the simulation experiment, a gust wind model dependent on a standard power spectral density is introduced, which is derived from the Dryden model [44], [45]. The spectrum of gust wind can be expressed as

$$\Phi_u (\omega) = \sigma_u^2 \frac{L_u}{\pi V_*} \frac{1}{1 + (L_u\omega/V_*)^2} \quad (32)$$

$$\Phi_v (\omega) = \sigma_v^2 \frac{L_v}{\pi V_*} \frac{1 + 12 (L_v\omega/V_*)^2}{\left(1 + 4 (L_v\omega/V_*)^2 \right)^2} \quad (33)$$

$$\Phi_w (\omega) = \sigma_w^2 \frac{L_w}{\pi V_*} \frac{1 + 12 (L_w\omega/V_*)^2}{\left(1 + 4 (L_w\omega/V_*)^2 \right)^2} \quad (34)$$

where σ_i and L_i are turbulence intensity and gust length scale. The vertical length scale and turbulence intensity can be assumed to be $L_w = h$ and $\sigma_w = 0.1\omega_{20}$. h is current altitude, ω_{20} is the given wind speed in knots at $20ft$ altitude. Then the horizontal turbulence intensities and gust length scales can be described as

$$L_u = L_v = \frac{h}{(0.177 + 0.000823)^{1.2}} \quad (35)$$

$$\sigma_u = \sigma_v = \frac{0.1\omega_{20}}{(0.177 + 0.000823h)^{0.4}} \quad (36)$$

Define the simulation time is 100s, $\omega_{20} = 10m/s$ and the hover height of the Tilt-rotor UAV is 40m, the gust wind in body frame calculated by Dryden model is shown in Figure 5.
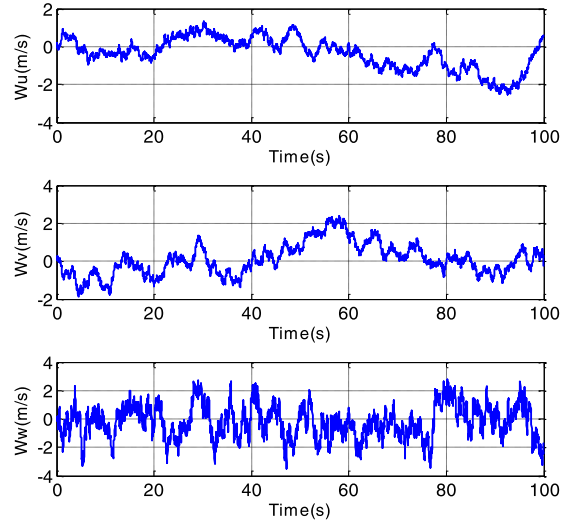
FIGURE 5. Simulation results of gust wind.
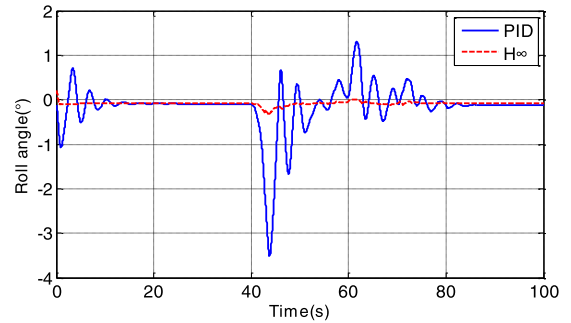
FIGURE 6. Comparison of roll angle control results.
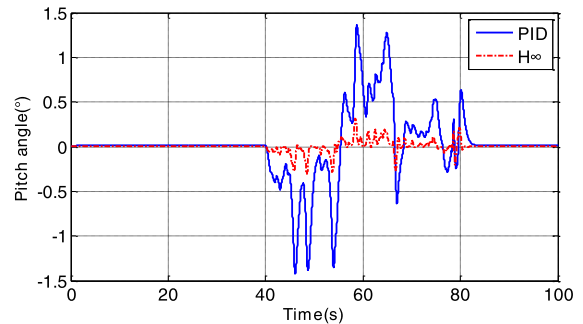
FIGURE 7. Comparison of pitch angle control results.

It is assumed that the Tilt-rotor UAV takes off vertically at 0s, and after 20s, it reaches 40m and keeps hovering. The gust wind is added in simulation model at $\Delta T = [40, 80] s$. The PID control method is introduced as a comparative experiment. The attitudes control results are shown in Figure 6~Figure 8.

As shown in Figure 6~Figure 8, it is clear that the $H\infty$ robust control method with mixed sensitivity has a good ability to suppress the wind field interference. Table 2 shows the mean square errors of control results.
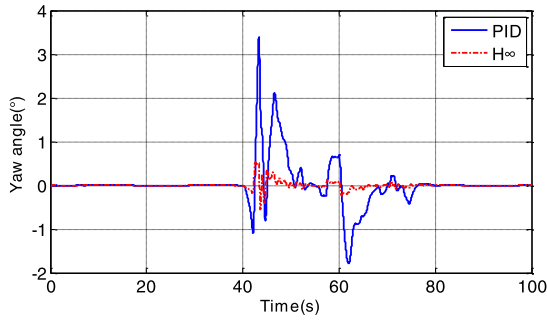
FIGURE 8. Comparison of yaw angle control results.

TABLE 2. The Mean Square Errors of Attitude Control Results.

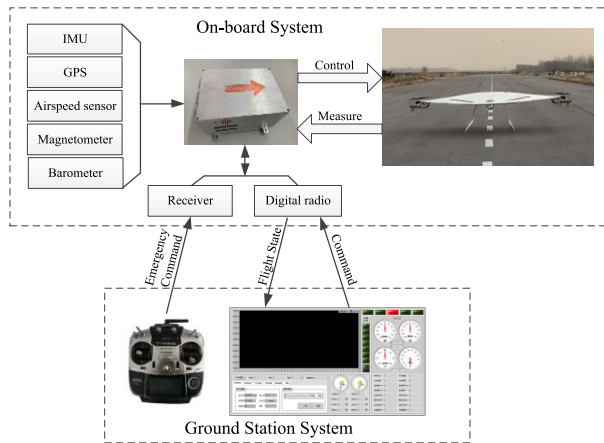| Attitude angles	Roll (°)	Pitch (°)	Yaw (°)
PID controller	0.5342	0.3800	0.4903
$H\infty$ controller	0.0408	0.0590	0.0793

FIGURE 9. Block diagram of the experiment system.

FIGURE 10. Hovering flight test photo.

B. ACTUAL FLIGHT VERIFICATION

In this part, a real flight experiment is carried out to verify the proposed method. The partial experimental settings are shown in Figure 9.

The experiment system consists of the on-board system and ground station system. The flight control system can measure the flight states through varies sensors, and give the control command to Tilt-rotor UAV. The transmitter can control the
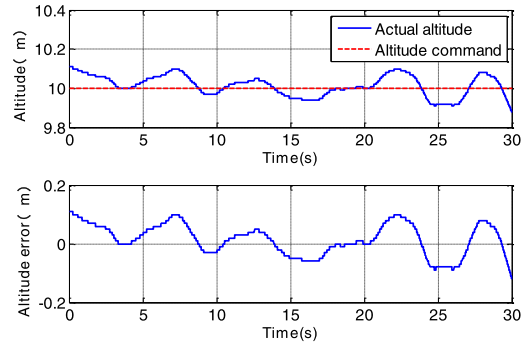

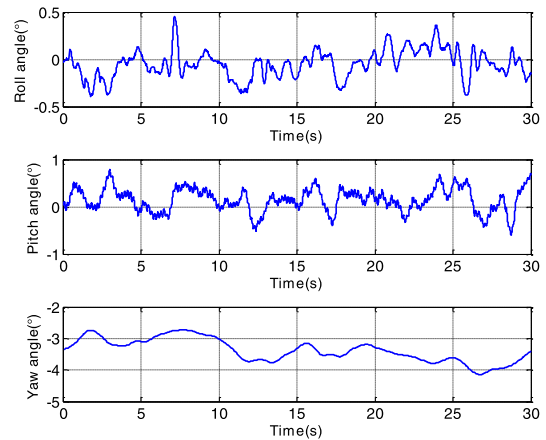**FIGURE 11.** The stability results of altitude control.

FIGURE 12. The stability results of attitude control.

UAV in an emergency. The ground display and control system communicates with flight control system through the digital radio.

As shown in Figure 10, the Tilt-rotor UAV takes off vertically and hovers at 10m altitude. The test results are illustrated in Figure 11 and Figure 12. It can be observed that the altitude error is kept within ± 0.2m. The error variation ranges of roll angle, pitch angle and yaw angle are basically within [−0.5°,0.5°], [−1°,1°] and [−4.5°, −2.5°], respectively. The attitude angles control results are consistent with the simulation results. Therefore, the proposed control method based on GESO and $H\infty$ robust control with mixed sensitivity could better deal with the wind field disturbance problem during vertical flight.

VI. CONCLUSION

In this article, a control method of Tilt-rotor UAV is proposed to resist wind disturbance. As the Tilt-rotor UAV has small airspeed during the take-off and landing phase, it is more susceptible to aerodynamic interference of wind field. The mechanism of wind disturbance is analyzed from two aspects of fuselage and propeller, and the wind disturbance is divided into external interference and modeling error and are added into the aerodynamic model. Taking into account the measurement noise of the MEMS sensors and the modeling error of wind field interference, a GESO is introduced to

estimate system states and total disturbances, and the stability of GESO is proved by Lyapunov theory. After that, a control method based on $H\infty$ robust control with mixed sensitivity is proposed, which could lead to good interference suppression ability and better performance tracking ability of the Tilt-rotor UAV. Simulation and experimental researches have been conducted to investigate the proposed control algorithm. As shown in the results, the proposed control method has a good ability to suppress the wind field interference and can achieve a better tracking effect with smaller steady errors.

The innovation of this article is to divide the influence of wind field into external disturbance and internal modeling error, then, the wind resistance control is realized by using $H\infty$ robust control with mixed sensitivity which is robust to external disturbance and internal modeling error. In addition, GESO is introduced to realize disturbance estimation and state estimation, which further improves the control accuracy.

REFERENCES

[1] J. Su, C. Su, S. Xu, and X. X. Yang, "A multibody model of tilt-rotor aircraft based on Kane's method," *Int. J. Aerosp. Eng.*, vol. 2019, Apr. 2019, Art. no. 9396352.

[2] J. C. Ho, B. Jayaraman, and H. Yeo, "Coupled computational fluid dynamics and comprehensive analysis calculations of a gimballed tiltrotor," *AIAA J.*, vol. 57, no. 10, pp. 4433–4446, Oct. 2019.

[3] R. Chiappinelli, M. Cohen, M. Doff-Sotta, M. Nahon, J. R. Forbes, and J. Apkarian, "Modeling and control of a passively-coupled tilt-rotor vertical takeoff and landing aircraft," in *Proc. Int. Conf. Robot. Autom. (ICRA)*, Montreal, QC, Canada, May 2019, pp. 4141–4147.

[4] A. Takii, M. Yamakawa, S. Asao, and K. Tjiri, "Six degrees of freedom numerical simulation of tilt-rotor plane," in *Proc. Int. Conf. Comput. Sci.*, Faro, Portugal, Jun. 2019, pp. 506–519.

[5] G. V. Raffo and M. M. D. Almeida, "A load transportation nonlinear control strategy using a tilt-rotor UAV," *J. Adv. Transp.*, vol. 2018, pp. 1–20, Jun. 2018.

[6] B. S. Rego and G. V. Raffo, "Suspended load path tracking control using a tilt-rotor UAV based on zonotopic state estimation," *J. Franklin Inst.*, vol. 356, no. 4, pp. 1695–1729, Mar. 2019.

[7] N. T. Hegde, V. I. George, C. G. Nayak, and K. Kumar, "Transition flight modeling and robust control of a VTOL unmanned quad tilt-rotor aerial vehicle," *Indonesian J. Elect. Eng. Comput. Sci.*, vol. 18, no. 3, pp. 1252–1261, Jun. 2020.

[8] Z. Liu, Y. He, L. Yang, and J. Han, "Control techniques of tilt rotor unmanned aerial vehicle systems: A review," *Chin. J. Aeronaut.*, vol. 30, no. 1, pp. 135–148, Feb. 2017.

[9] Z. Wu, C. Li, and Y. Cao, "Numerical simulation of rotor–Wing transient interaction for a tiltrotor in the transition mode," *Mathematics*, vol. 7, no. 2, p. 116, Jan. 2019.

[10] P. Li, Q. Zhao, and Q. Zhu, "CFD calculations on the unsteady aerodynamic characteristics of a tilt-rotor in a conversion mode," *Chin. J. Aeronaut.*, vol. 28, no. 6, pp. 1593–1605, Dec. 2015.

[11] J. E. Wakefield, D. P. Jones, A. Gaitonde, and S. Medina, "Coupled flight mechanics based on reduced order models for use in tiltrotor stability analysis," in *Proc. AIAA Aviation Forum*, Jun. 2019, pp. 1–30.

[12] S. Choi, Y. Kang, S. Chang, S. Koo, and J. M. Kim, "Development and conversion flight test of a small tiltrotor unmanned aerial vehicle," *J. Aircr.*, vol. 47, no. 2, pp. 730–732, Mar. 2010.

[13] T. Lombaerts, J. Kaneshige, S. Schuet, G. Hardy, B. L. Aponso, and K. H. Shish, "Nonlinear dynamic inversion based attitude control for a hovering quad tiltrotor eVTOL vehicle," in *Proc. AIAA Scitech Forum*, San Diego, CA, USA, Jan. 2019, pp. 1–26.

[14] Z. Chen and H. Jia, "Design of flight control system for a novel tilt-rotor UAV," *Complexity*, vol. 2020, Mar. 2020, Art. no. 4757381.

[15] Z. Lyu, Z. Wang, D. Duan, L. Lin, J. Li, Y. Yang, Y. Chen, and Y. Li, "Tilting path optimization of tilt quad rotor in conversion process based on ant colony optimization algorithm," *IEEE Access*, vol. 8, pp. 140777–140791, 2020.

[16] M. Alam, S. Celikovsky, and D. Walker, "Robust hover mode control of a tiltrotor using nonlinear control technique," in *Proc. AIAA Guid., Navigat., Control Conf.*, San Diego, CA, USA, Jan. 2016, pp. 1–16.

[17] G. Di Francesco and M. Mattei, "Modeling and incremental nonlinear dynamic inversion control of a novel unmanned tiltrotor," *J. Aircr.*, vol. 53, no. 1, pp. 73–86, Jan. 2016.

[18] J. Zhang, L. Sun, X. J. Qu, and L. P. Wang, "Time-varying linear control for tiltrotor aircraft," *Chin. J. Aeronaut.*, vol. 31, no. 4, pp. 632–642, Apr. 2018.

[19] C. Papachristos, K. Alexis, and A. Tzes, "Dual–authority thrust–vectoring of a tri–tiltrotor employing model predictive control," *J. Intell. Robotic Syst.*, vol. 81, pp. 471–504, May 2016.

[20] C. Papachristos, K. Alexis, G. Nikolakopoulos, and A. Tzes, "Model predictive attitude control of an unmanned tilt-rotor aircraft," in *Proc. IEEE Int. Symp. Ind. Electron.*, Gdansk, Poland, Jun. 2011, pp. 922–927.

[21] G. Notarstefano and J. Hauser, "Modeling and dynamic exploration of a tilt-rotor VTOL aircraft," in *Proc. 8th IFAC Symp. Nonlinear Control Syst.* Bologna, Italy: Univ. Bologna, Sep. 2010, pp. 119–124.

[22] K. Benkhoud and S. Bouallègue, "Dynamics modeling and advanced metaheuristics based LQG controller design for a quad tilt wing UAV," *Int. J. Dyn. Control*, vol. 6, no. 2, pp. 630–651, Jun. 2018.

[23] G.-B. Wang, "Adaptive sliding mode robust control based on multidimensional Taylor network for trajectory tracking of quadrotor UAV," *IET Control Theory Appl.*, vol. 14, no. 14, pp. 1855–1866, Sep. 2020.

[24] A. Guendouzi, M. Hamerlain, and N. Saadia, "A robust adaptive nonlinear control design via geometric approach for a quadrotor," *IETE J. Res.*, to be published.

[25] F. Chen, R. Jiang, K. Zhang, B. Jiang, and G. Tao, "Robust backstepping sliding-mode control and observer-based fault estimation for a quadrotor UAV," *IEEE Trans. Ind. Electron.*, vol. 63, no. 8, pp. 5044–5056, Aug. 2016.

[26] S. R. Bassolillo, E. D. Amato, I. Notaro, L. Blasi, and M. Mattei, "Decentralized mesh-based model predictive control for swarms of UAVs," *Sensors*, vol. 20, no. 15, p. 4324, Aug. 2020.

[27] N. Liu, Z. Cai, J. Zhao, and Y. Wang, "Predictor-based model reference adaptive roll and yaw control of a quad-tiltrotor UAV," *Chin. J. Aeronaut.*, vol. 33, no. 1, pp. 282–295, Jan. 2020.

[28] O. Doukhi and D. J. Lee, "Neural network-based robust adaptive certainty equivalent controller for quadrotor UAV with unknown disturbances," *Int. J. Control, Autom. Syst.*, vol. 17, no. 9, pp. 2365–2374, Sep. 2019.

[29] B.-M. Kim, B. S. Kim, and N.-W. Kim, "Trajectory tracking controller design using neural networks for a tiltrotor unmanned aerial vehicle," *Proc. Inst. Mech. Eng., G, J. Aerosp. Eng.*, vol. 224, no. 8, pp. 881–896, Aug. 2010.

[30] Q. Xu, Z. Wang, and Z. Zhen, "Adaptive neural network finite time control for quadrotor UAV with unknown input saturation," *Nonlinear Dyn.*, vol. 98, no. 3, pp. 1973–1998, Oct. 2019.

[31] H. Razmi and S. Afshinfar, "Neural network-based adaptive sliding mode control design for position and attitude control of a quadrotor UAV," *Aerosp. Sci. Technol.*, vol. 91, pp. 12–27, Aug. 2019.

[32] S. Wang, B. Song, L. He, and X. Lang, "Modeling and robust attitude controller design of a distributed propulsion tilt-wing UAV in hovering flight," in *Proc. Chin. Control Decis. Conf. (CCDC)*, Nanchang, China, Jun. 2019, pp. 1480–1485.

[33] Z. Yao and S. Wu, "Intermittent gliding flight control design and verification of a morphing unmanned aerial vehicle," *IEEE Access*, vol. 7, pp. 40991–41005, 2019.

[34] C. Liu, B. Jiang, and K. Zhang, "Adaptive fault-tolerant H-Infinity output feedback control for Lead–Wing close formation flight," *IEEE Trans. Syst., Man, Cybern. Syst.*, vol. 50, no. 8, pp. 2804–2814, Aug. 2020.

[35] M. A. Lotufo, L. Colangelo, and C. Novara, "Control design for UAV quadrotors via embedded model control," *IEEE Trans. Control Syst. Technol.*, vol. 28, no. 5, pp. 1741–1756, Sep. 2020.

[36] H. Li and J. Yu, "Anti-disturbance control based on cascade ESO and sliding mode control for gimbal system of double gimbal CMG," *IEEE Access*, vol. 8, pp. 5644–5654, 2020.

[37] S. Y. Jung and Y. D. Kim, "Extended state observer-based robust pitch autopilot design for small UAV," in *Proc. 18th Int. Conf. Control, Automat. Syst. (ICCAS)*, Daegwallyeong, South Korea, Oct. 2018, pp. 433–438.

[38] R. Mu, J. Chen, K. Peng, X. Zhang, Y. Deng, and N. Cui, "Finite-time super-twisting controller based on SESO design for RLV re-entry phase," *IEEE Access*, vol. 7, pp. 37371–37380, 2019.

[39] L. Zhou and J. She, "Generalized-Extended-State-Observer-Based repetitive control for MIMO systems with mismatched disturbances," *IEEE Access*, vol. 6, pp. 61377–61385, 2018.

[40] D. Shi, Z. Wu, and W. Chou, "Generalized extended state observer based high precision attitude control of quadrotor vehicles subject to wind disturbance," *IEEE Access*, vol. 6, pp. 32349–32359, 2018.

[41] X. Y. Zhang, S. Q. Zhang, Z. X. Wang, X. S. Qin, R. S. Wang, and R. Schmidt, "Disturbance rejection control with H_∞ optimized observer for vibration suppression of piezoelectric smart structures," *Mech. Ind.*, vol. 20, no. 2, pp. 1–13, Feb. 2019.

[42] F. H. D. Guaracy, L. H. C. Ferreira, and C. A. M. Pinheiro, "The discrete-time controller for the H_∞/LTR problem with mixed-sensitivity properties," *Automatica*, vol. 25, pp. 28–31, Aug. 2015.

[43] N. S. Ahmad, "Robust H_∞-fuzzy logic control for enhanced tracking performance of a wheeled mobile robot in the presence of uncertain nonlinear perturbations," *Sensors*, vol. 20, no. 13, p. 3673, Jun. 2020.

[44] S. Waslander and C. Wang, "Wind disturbance estimation and rejection for quadrotor position control," in *Proc. AIAA Infotech@Aerospace Conf.*, Seattle, WA, USA, Apr. 2009, pp. 1–14.

[45] P. P. Neumann and M. Bartholmai, "Real-time wind estimation on a micro unmanned aerial vehicle using its inertial measurement unit," *Sens. Actuators A, Phys.*, vol. 235, pp. 300–310, Nov. 2015.

JINGJUAN ZHANG received the B.S. and Ph.D. degrees from Harbin Engineering University, in 2001 and 2003, respectively.

She is currently a Professor with the School of Instrumentation and Optoelectronic Engineering, Beihang University. Her current research interests include inertial navigation, integrated navigation systems, and aircraft cooperative control technology.

XUEYUN WANG received the B.S. and Ph.D. degrees from the School of Instrumentation and Optoelectronic Engineering, Beihang University, in 2011 and 2016, respectively.

He is currently a Lecturer with the School of Instrumentation and Optoelectronic Engineering, Beihang University. His current research interests include inertial navigation, integrated navigation systems, and aircraft cooperative control technology.

YIFAN XU received the B.S. degree from the School of Instrumentation and Optoelectronic Engineering, Beihang University, in 2017, where he is currently pursuing the Ph.D. degree. His current research interests include integrated navigation and flight control.

QIAN ZHANG received the B.S. and Ph.D. degrees from the School of Instrumentation and Optoelectronic Engineering, Beihang University, in 2012 and 2019, respectively.

He currently holds a postdoctoral position with the School of Aeronautic Science and Engineering, Beihang University. His current research interests include inertial navigation, unmanned aerial vehicles design, control and integrated navigation, and fault detection and diagnosis.

ZELONG YU received the B.S. degree from the School of Instrumentation and Optoelectronic Engineering, Beihang University, in 2016, where he is currently pursuing the Ph.D. degree. His current research interests include integrated navigation and flight control.

● ● ●